INFLUENCE OF FLOW MODELS IN AN AEROELASTIC PROBLEM: COMPARISON OF A TURBULENCE MODEL WITH A LAMINAR SOLUTION OF THE NAVIER-STOKES EQUATIONS

P. Sváček

Czech Technical University Prague, Faculty of Mechanical Engineering, Karlovo nám. 13, 121 35 Praha 2, Czech Republic

M. Feistauer

Charles University Prague, Faculty of Mathematics and Physics, Sokolovská 83, 186 75 Praha 8, Czech Republic

J. Horáček

Institute of Thermomechanics, Academy of Sciences of the Czech Republic, Dolejškova 5, 182 00 Praha 8, Czech Republic

ABSTRACT

The study deals with numerical approximation of a 2D aeroelastic problem. A fully coupled formulation of flow over a freely vibrating airfoil with two degrees of freedom for rotation and translation is considered. The flow is described by the incompressible Navier-Stokes equations written in Arbitrary Lagrangian-Eulerian (ALE) form or by the Reynolds averaged Navier-Stokes system. The flow is solved by the stabilized finite element method. The developed method is verified by experimental data and the numerical results obtained for laminar and turbulent models are compared.

1. INTRODUCTION

In many technical disciplines the interaction of fluid flow and an vibrating structure plays an important role. [see, e.g., Dowell (1995)]. During last years, significant advances have been made in the development of computational methods for simulation of the fluid-structure interaction, see, e.g., Bathe (2007). In the present study the main attention is paid to the comparison of numerical simulations of free airfoil NACA0012 vibrations with large amplitudes in turbulent and laminar flows.

The authors acknowledge the financial support of the Grant Agency of Academy of Sciences of the Czech Republic by the project No. IAA200760613 "Computer Modelling of Aeroelastic Phenomena for Real Fluid Flowing past Vibrating Airfoils Particularly after the Loss of System Stability". The research was partially supported research plans MSM 0021620839 (M. Feistauer), MSM 6840770003 (P. Sváček) of the Ministry of Education of the Czech Republic.

2. MATHEMATICAL MODELS

The mathematical analysis consists of the flow and structure models and the coupling conditions. Here we study the interaction of fluid and a flexibly supported airfoil, which can be vertically displaced and rotated around its elastic axis. The character of the flow depends on the magnitude of the Reynolds number: for a sufficiently small Reynolds number the flow is laminar but with increasing Reynolds numbers it becomes turbulent. Here, the two different flow models are considered. The motion of the airfoil is described by the two nonlinear equations of motion. The flow and structure models are then coupled by the kinematic and dynamic conditions.

2.1. Laminar model

First, we introduce the flow model for the laminar case, which is described by the incompressible Navier-Stokes equations. In order to treat the domain motion due to the structural deformations the ALE method is applied. The Navier-Stokes system written in ALE form then reads

$$\begin{aligned} \frac{D^{\mathcal{A}} v_i}{Dt} + (\mathbf{v} - \mathbf{w}_D) \cdot \nabla v_i + \frac{\partial p}{\partial x_i} \\ = \sum_{j=1}^{2} \frac{\partial}{\partial x_j} \left(\nu \Big(\frac{\partial v_i}{\partial x_j} + \frac{\partial v_j}{\partial x_i} \Big) \right) \text{ in } \Omega_t, \qquad (1) \\ \nabla \cdot \mathbf{v} = 0 \text{ in } \Omega_t, \end{aligned}$$

where $\frac{D^{\mathcal{A}}}{Dt}$ denotes the ALE derivative, $\mathbf{w}_D$ denotes the ALE domain velocity, $\mathbf{v} = (v_1, v_2)^T$

is the velocity vector, p is the kinematic pressure, and ν is the kinematic viscosity. The symbol $\mathcal{A}_t$ denotes a regular one-to-one Arbitrary Lagrangian-Eulerian (ALE) mapping of the reference configuration Ω_0 onto the current configuration Ω_t for any time instant $t \in [0, T]$. The system of equations (1) is equipped with suitable boundary and initial conditions, cf. Sváček and Feistauer (2004). On the moving part of boundary (airfoil surface Γ_{Wt}) the kinematic boundary condition is prescribed, i.e. $\mathbf{v} = \mathbf{w}_D$ on Γ_{Wt}.

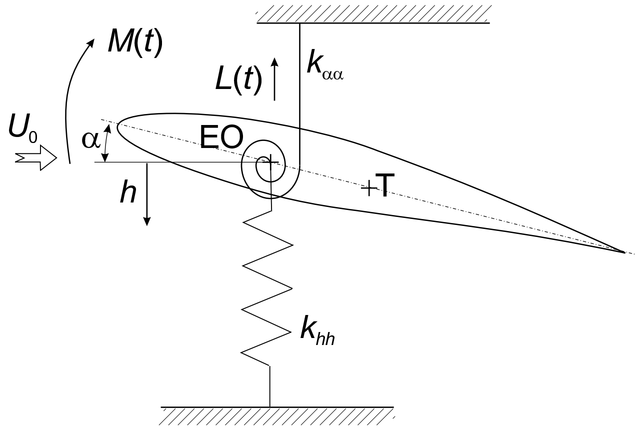

Figure 1: The elastic support of the airfoil on translational and rotational springs.

2.2. Turbulence model

In the case of high Reynolds numbers the flow becomes turbulent. In order to numerically approximate the turbulent flow one possibility is to model only mean parts of aerodynamical quantities. The influence of fluctuating parts is modelled with the aid of the Boussinesq assumption. Starting from the Navier-Stokes equations, the velocity $\mathbf{v}$ is decomposed into the mean part $\mathbf{V}$ and the fluctuating part $\mathbf{v}'$, i.e. $\mathbf{v} = \mathbf{V} + \mathbf{v}'$ with its components $v_i = V_i + v_i'$. Similarly, the kinematic pressure p is decomposed into the mean part P and the fluctuating part p', i.e. $p = P + p'$. The Reynolds Averaged Navier-Stokes (RANS) equations read

$$\begin{aligned} &\frac{D^{\mathcal{A}t} v_i}{Dt} + ((\mathbf{v} - \mathbf{w}_D) \cdot \nabla) v_i + \frac{\partial p}{\partial x_i} \\ &-\frac{\partial}{\partial x_j} \left((\nu + \nu_T) \Big(\frac{\partial v_i}{\partial x_j} + \frac{\partial v_j}{\partial x_i} \Big) \right) = 0 \text{ in } \Omega_t, \quad (2) \\ &\nabla \cdot \mathbf{v} = 0 \text{ in } \Omega_t, \end{aligned}$$

where ν_T is the turbulent viscosity, which requires further modelling. The system of equations (1) is equipped with suitable boundary and initial conditions, cf. Sváček, P. *et al.* (2005).

The turbulent viscosity ν_T is computed with the aid of the Spalart-Allmaras model, represented by the equation

$$\begin{aligned} &\frac{D^{\mathcal{A}t} \widetilde{\nu}}{Dt} + (\mathbf{v} - \mathbf{w}_D) \cdot \nabla \widetilde{\nu} = G(\widetilde{\nu}) - Y(\widetilde{\nu}) \quad (3) \\ &+\frac{1}{\beta} \left[\sum_{i=1}^{2} \frac{\partial}{\partial x_i} \left((\nu + \widetilde{\nu}) \frac{\partial \widetilde{\nu}}{\partial x_i} \right) + c_{b_2} (\nabla \widetilde{\nu})^2 \right], \end{aligned}$$

for an additional quantity $\widetilde{\nu}$. Here the functions $G(\widetilde{\nu})$ and $Y(\widetilde{\nu})$ are functions of the tensor $(\omega_{ij})_{ij}$ of rotation of the mean velocity and of the wall distance y. Here, the components of the rotation tensor are defined by $\omega_{ij} = \frac{1}{2} \left(\frac{\partial V_j}{\partial x_j} - \frac{\partial V_j}{\partial x_i} \right)$. The turbulent viscosity ν_T is defined by

$$\nu_T = \widetilde{\nu} \frac{\chi^3}{\chi^3 + c_v^3}, \qquad \chi = \frac{\widetilde{\nu}}{\nu}. \quad (4)$$

We use the following relations (see also Wilcox (1993)) $G(\widetilde{\nu}) = c_{b_1} \widetilde{S} \widetilde{\nu}$, $f_{v_2} = 1 - \frac{\chi}{1 + \chi f_{v_1}}$, $g = r + c_{w_2}(r^6 - r)$, $r = \frac{\widetilde{\nu}}{\widetilde{S} \kappa^2 y^2}$, $S = \sqrt{2 \sum_{i,j} \omega_{ij}^2}$,

$$Y = c_{w_1} \frac{\widetilde{\nu}^2}{y^2} \left(\frac{1 + c_{w_3}^6}{1 + c_{w_3}^6 / g^6} \right)^{\frac{1}{6}}, \ \widetilde{S} = S + \frac{\widetilde{\nu}}{\kappa^2 y^2} f_{v_2},$$

and y denotes the distance from a wall. The following choice of constants is used: $c_{b_1} = 0.1355$, $c_{b_2} = 0.622$, $\beta = \frac{2}{3}$, $c_v = 7.1$, $c_{w_2} = 0.3$, $c_{w_3} = 2.0$, $\kappa = 0.41$, $c_{w_1} = c_{b_1}/\kappa^2 + (1 + c_{b_2})/\beta$.

2.3. Structural model

Here, a solid flexibly supported airfoil is considered. The airfoil can be vertically displaced and rotated. Fig. 1 shows the elastic support of the airfoil on translational and rotational springs. The pressure and viscous forces acting on the vibrating airfoil immersed in flow result in the lift force $L(t)$ and the torsional moment $M(t)$. The governing nonlinear equations are written in the form (see Sváček *et al.* (2007))

$$\begin{aligned} m\ddot{h} + S_\alpha \ddot{\alpha} \cos\alpha - S_\alpha \dot{\alpha}^2 \sin\alpha + k_{hh} h &= -L(t), \\ S_\alpha \ddot{h} \cos\alpha + I_\alpha \ddot{\alpha} + k_{\alpha\alpha} \alpha &= M(t), \end{aligned}$$

where k_{hh} and $k_{\alpha\alpha}$ are the bending stiffness and torsional stiffness, respectively, m is the mass of the airfoil, S_α is the static moment around the elastic axis EO and I_α is the inertia moment around EO.

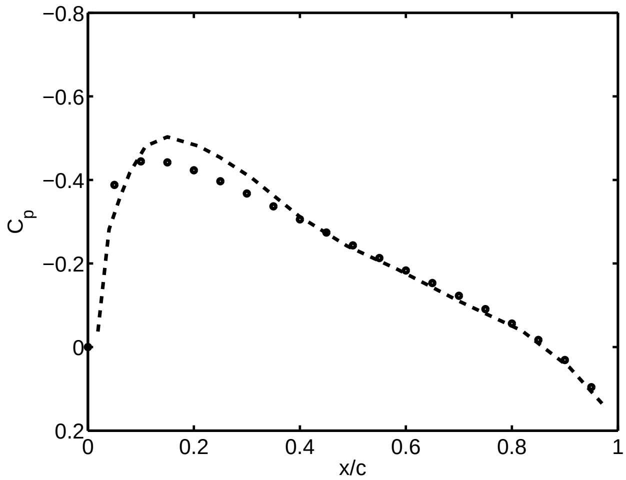

Figure 2: Distribution of the pressure coefficient c_p on the surface of the airfoil NACL 0012 obtained from the numerical simulations by the turbulence model (stationary solution): computed values, ∘; experimental data, — —.

3. NUMERICAL APPROXIMATION

In order to solve the problem numerically, we first start with the time discretization of the flow model. The ALE derivative is approximated by a two step backward difference formula. The problem discretized in time is solved by the finite element method. The construction of the finite element space is based on a triangulation of a polygonal approximation of the computational domain (denoted again by Ω).

3.1. Flow problem

It is well-known that FEM can be applied with success to a large variety of problems. However, in the finite element solution of incompressible Navier-Stokes equations several important obstacles need to be overcome. First, it is necessary to take into account that the finite element velocity/pressure pair has to be suitably chosen in order to satisfy the Babuška-Breezi condition, which guarantees the stability of the scheme – see, e.g., Girault and Raviart (1986). In practical computations we assume that the domain Ω is a polygonal approximation of the region occupied by the fluid at time t and the finite element spaces are defined over a triangulation $\mathcal{T}_\Delta$ of the domain Ω, formed by a finite number of closed triangles $K \in \mathcal{T}_\Delta$. In our computations, the well-known Taylor-Hood P_2/P_1 conforming elements are used for the velocity/pressure approximation. This means that the finite element approximation of the pressure p_Δ is a piecewise linear function and the approximation of the velocity $\mathbf{v}_\Delta$ is a piecewise quadratic vector-valued function on each element $K \in \mathcal{T}_\Delta$.

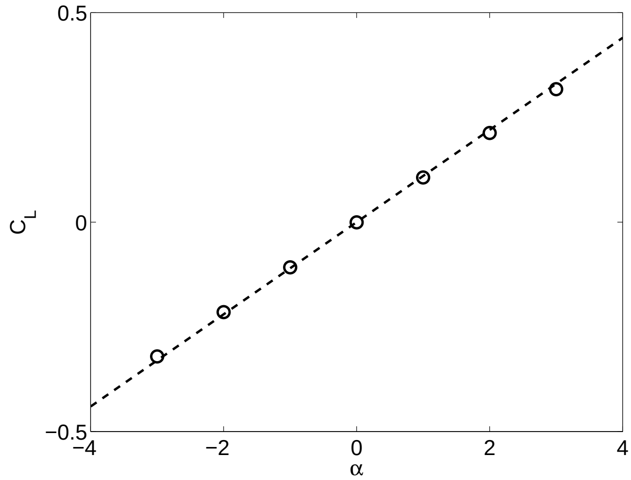

Figure 3: Comparison of the experimental lift coefficient and the lift coefficient computed by the finite element method (turbulence model): computed values, ∘; experimental data, — —.

Furthermore, the standard Galerkin discretization may produce approximate solutions suffering from spurious oscillations for high Reynolds numbers. In order to avoid this drawback, the *stabilization via streamline-diffusion/Petrov-Galerkin technique* is applied [see, e.g., Gelhard *et al.* (2005), Sváček *et al.* (2007)]. Moreover, it is necessary to design carefully the computational mesh, using adaptive grid refinement in order to allow an accurate resolution of time oscillating thin boundary layers, wakes and vortices. In our case we use the anisotropic mesh adaptation technique by Dolejší (2001) for the construction and adaptive refinement of the mesh.

3.2. Spalart-Allmaras model

In order to approximate the problem (3) we use the finite element space of the piecewise linear functions. The Galerkin approximations do not guarantee the monotonicity of the solution, but the function $\widetilde{\nu}$ needs to preserve positivity. The ELS/SUNG stabilization introduced in Sváček *et al.* (2007) provides enough streamline diffusion to stabilize the scheme, but still local oscillations leading to possible negative values of the variable $\widetilde{\nu}$ can appear. The additional artificial viscosity stabilizing procedure based on crosswind diffusion is introduced, cf. Codina (1993).

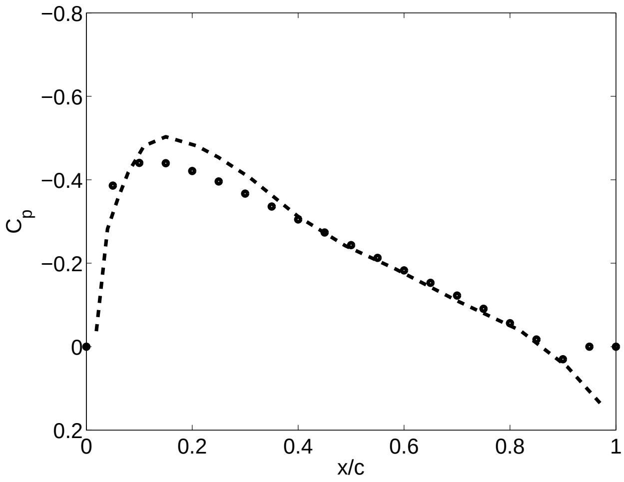

Figure 4: The distribution of the pressure mean coefficient c_p on the airfoil surface (turbulence model,vibrating airfoil NACA 0012): computed values, ∘; experimental data, — —.

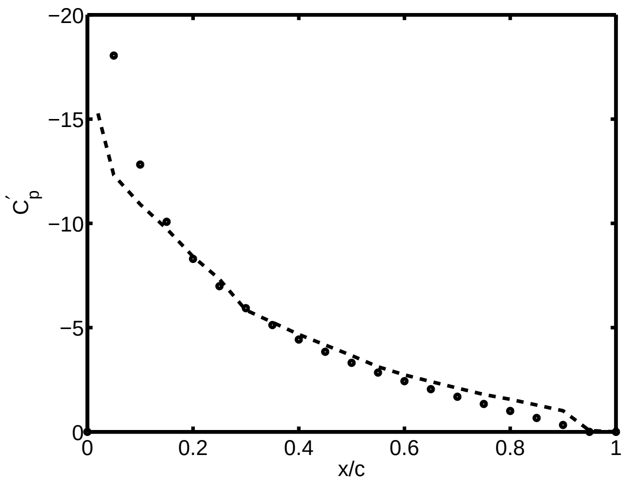

Figure 5: The distribution of the real part c_p' of the pressure coefficient on the airfoil surface (turbulence model,vibrating airfoil NACA 0012): computed values, ∘; experimental data, — —.

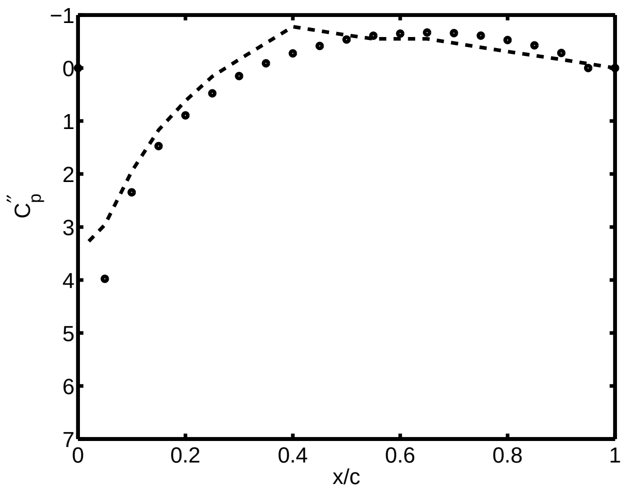

Figure 6: The distribution of the imaginary part c_p'' of the pressure coefficient on the airfoil surface (turbulence model,vibrating airfoil NACA 0012): computed values, ∘; experimental data, — —.

4. NUMERICAL RESULTS

First, the validation of the turbulence model was performed for flow over NACA 0012 airfoil. The approximation of the stationary turbulent flow was computed and the distribution of the pressure coefficient $c_p = (p - p_\infty)/(1/2\rho U_\infty^2)$ over the surface of the airfoil was compared with the mean values from Benetka and Horáček (2003), see Fig. 2. The lift coefficient in dependence on the angle of attack is compared in Fig. 3 with the data of Sheldahl and Klimas (1981). Further, the numerical approximation of flow over airfoil NACA 0012 for prescribed harmonic airfoil vibrations was compared to the measurement, see Benetka and Horáček (2003). The comparison is shown in Figs. 4-6.

The turbulent and laminar approaches were compared on the aeroelastic computations for the NACA 0012 airfoil with the parameters as in Sváček *et al.* (2007). The results are shown in Figs. 7– 12 for three oncoming airflow velocities. The numerical simulations for the turbulent flow were performed on anisotropically refined mesh with 27376 elements and 13850 vertices. The number of total unknowns was approximately 120000. The mesh was refined in the boundary layer region in order to capture both the laminar, logarithmic and the turbulent sublayers (no wall functions were used). The laminar flow was approximated with the aid of the mesh with 21994 elements and 11169 vertices (total number of unknowns was about 100000). The same time step values were chosen for both the laminar and turbulent computations ($\Delta t U_\infty / L_\infty = 0.0025$).

5. CONCLUSIONS

The method developed for the numerical simulation of airfoil aeroelastic behaviour in turbulent flow was successfully validated by experimental data known for stationary and fixed profile NACA 0012 and for prescribed torsional airfoil vibration. For low oncoming airflow velocities, the vibrations are damped by aerodynamic forces and the system is stable. Small sustained airfoil vibrations for the laminar flow are caused by vortices periodically shedding from the profile, in contrast to the turbulent flow, where the vibration level decay is much stronger (see Figs. 7 and 8). For higher flow velocities (see Figs. 9-12) near the instability threshold the tendencies in the displacements of the airfoil in time domain are similar for turbulent and laminar flows. The system becomes unstable by divergence for translation at about 37.7 m/s, followed by flutter for rotation above the flow velocity 42.4 m/s (see Sváček *et al.* (2007)).

6. REFERENCES

Bathe, K. J., (ed.), 2007, Computational Fluid and Solid Mechanics 2007. Elsevier.

Benetka, J., Horáček, J., 2003 , Experimental pressure data on vibrating airfoils NACA 64A012M5 and NACA 0012. Technical report, Institute of Thermomechanics, Czech Academy of Sciences.

Codina, R., 1993, A discontinuity capturing crosswind-dissipation for the finite element solution of the convection diffusion equation. *Computational Methods in Applied Mechanical Engineering*, **110**, 325–342.

Dolejší, V., 2001, Anisotropic mesh adaptation technique for viscous flow simulation. *East-West Journal of Numerical Mathematics*, **9**: 1–24.

Dowell, E. H., 1995, A Modern Course in Aeroelasticity. Kluwer Academic Publishers, Dodrecht.

Gelhard, T., Lube, G., Olshanskii, M. A., Starcke, J.-H., 2005, Stabilized finite element schemes with LBB-stable elements for incompressible flows. *Journal of Computational and Applied Mathematics*, **177**:243–267.

Girault, V., Raviart, P.-A., 1986, *Finite Element Methods for the Navier-Stokes Equations*. Springer-Verlag, Berlin.

Sheldahl, R. E., Klimas, P. C., 1981, Aerodynamic characteristics of seven airfoil sections through 180 degrees angle of attack for use in aerodynamic analysis of vertical axis wind turbines. Tech. Rep. SAND80-2114, Sandia Nat. Lab., New Mexico.

Sváček, P., Feistauer, M., 2004, Application of a Stabilized FEM to Problems of Aeroelasticity. In *Numerical Mathematics and Advanced Application*, pages 796–805, Berlin. Springer.

Sváček, P., Feistauer, M., Horáček, J., 2007 , Numerical simulation of flow induced airfoil vibrations with large amplitudes. *Journal of Fluids and Structure*, **23**(3):391–411.

Sváček, P. , Feistauer, M., and Horáček, J., 2005, Numerical modelling of flow induced airfoil vibrations problem. In *Int. Conf. Innovation Integration in Aerospace Sciences [CD-ROM]*, page 10 pp., CEIAT, Queen's University Belfast.

Wilcox, D. C., 1993, Turbulence Modeling for CFD. DCW Industries.

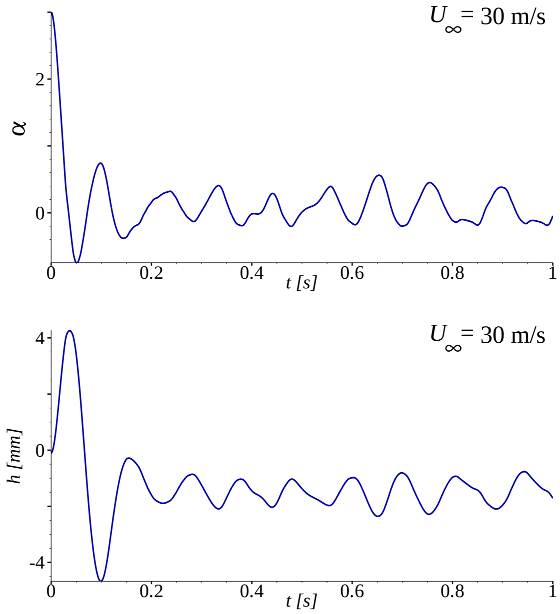

Figure 7: Aeroelastic response for laminar model and $U_\infty = 30\ \mathrm{m\,s^{-1}}$

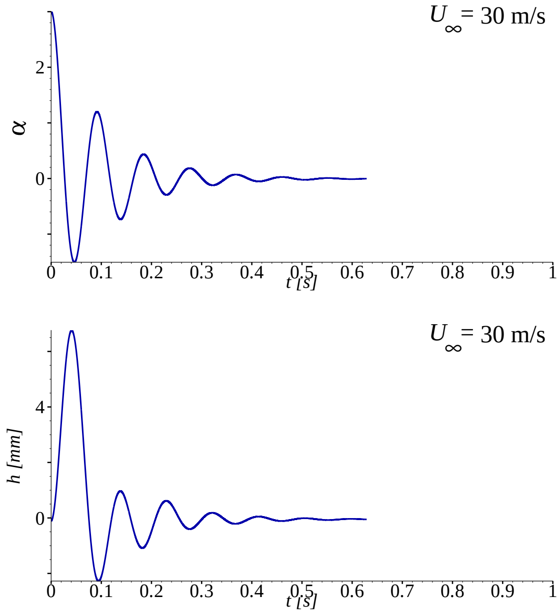

Figure 8: Aeroelastic response for turbulence model and $U_\infty = 30\ \mathrm{m\,s^{-1}}$

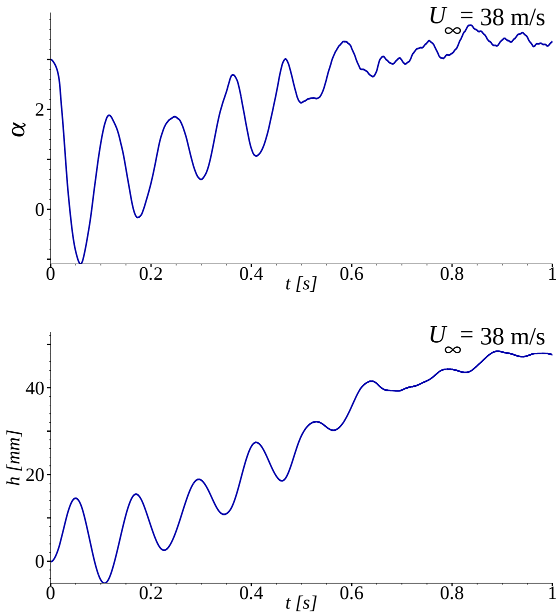

Figure 9: Aeroelastic response for laminar model and $U_\infty = 38\ \mathrm{m\,s^{-1}}$

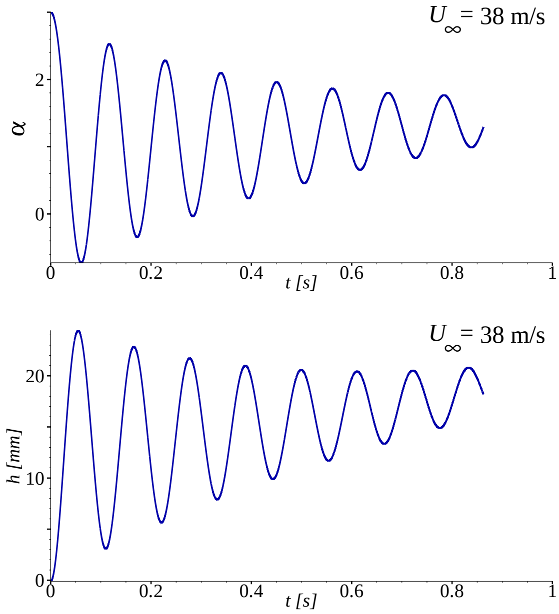

Figure 10: Aeroelastic response for turbulence model and $U_\infty = 38\ \mathrm{m\,s^{-1}}$

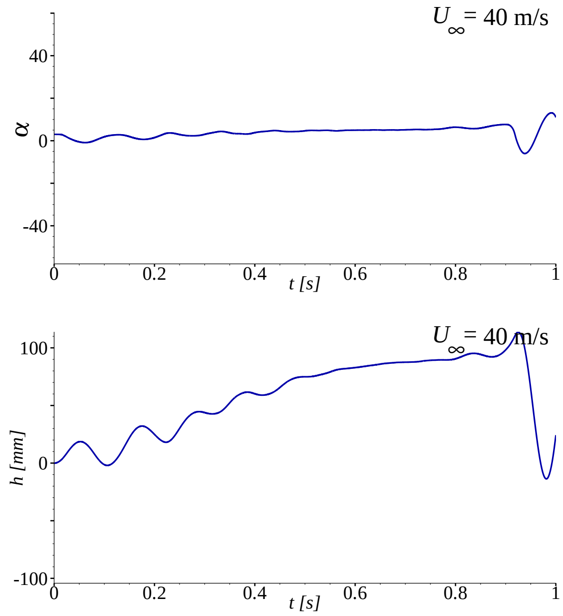

Figure 11: Aeroelastic response for laminar model and $U_\infty = 40\ \mathrm{m\,s^{-1}}$

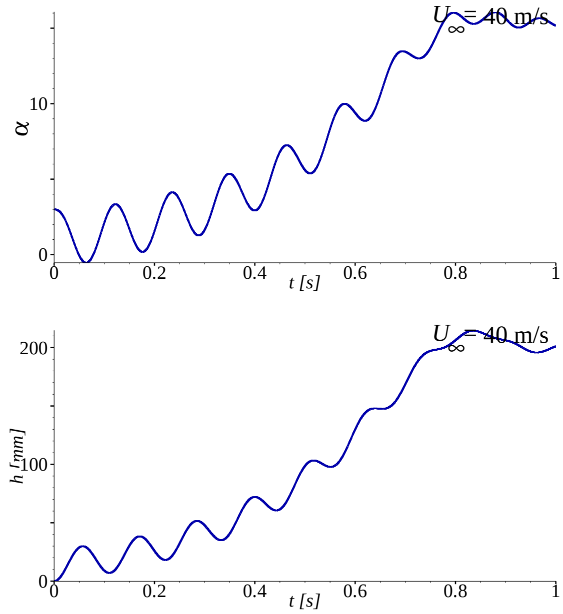

Figure 12: Aeroelastic response for turbulence model and $U_\infty = 40\ \mathrm{m\,s^{-1}}$